Experimental Neurology **156,** 394–406 (1999)
Article ID exnr.1999.7033, available online at http://www.idealibrary.com on IDEAL®

Imaging Cells in the Developing Nervous System with Retrovirus Expressing Modified Green Fluorescent Protein

Ami Okada,*,[1] Rusty Lansford,† James M. Weimann,* Scott E. Fraser,† and Susan K. McConnell*

**Department of Biological Sciences, Stanford University, Stanford, California 94305; and †Biological Imaging Center, California Institute of Technology, Pasadena, California 91125*

Received October 26, 1998; accepted November 30, 1998

To visualize the movements of cells and their processes in developing vertebrates, we constructed replication-incompetent retroviral vectors encoding green fluorescent protein (GFP) that can be detected as a single integrated copy per cell. To optimize GFP expression, the CMV enhancer and avian β-actin promoter were incorporated within a retrovirus construct to drive transcription of redshifted (F64L, S65T) and codon-modified GFP (EGFP), EGFP tagged with GAP-43 sequences targeting the GFP to the cell membrane, or EGFP with additional mutations that increase its ability to fold properly at 37°C (S147P or V163A, S175G). We have used these viruses to efficiently mark and follow the developmental progression of a large population of cells in rat neocortex and whole avian embryos. In the chick embryo, the migration and development of GFP-marked neural crest cells were monitored using time-lapse videomicroscopy. In the neocortex, GFP clearly delineates the morphology of a variety of neuronal and glial phenotypes. Cells expressing GFP display normal dendritic morphologies, and infected cells persist into adulthood. Cortical neurons appear to form normal local axonal and long-distance projections, suggesting that the presence of cytoplasmic or GAP-43-tagged GFP does not significantly interfere with normal development. © 1999 Academic Press

Key Words: **GFP; retrovirus; vesicular stomatitis virus G protein; neural development; imaging; cerebral cortex; cell lineage.**

INTRODUCTION

Studies of nervous system development would benefit from the ability to easily observe the morphology or movement of individual cells. In recent years, the use of green fluorescent protein (GFP) from the jellyfish *Aequorea* has revolutionized our ability to visualize biological events. Because the fluorescent chromophore in GFP is encoded by the primary structure of the protein (reviewed in 37, 43), the addition of substrates is not required for the detection of GFP, and the expression of GFP in cells of interest allows the direct and continuous imaging of live cells by epifluorescence. In contrast with common methods of fluorescently labeling cells (e.g., lipophilic carbocyanine vital dyes such as DiI), GFP protein remains in a cell and its progeny as long as the vector remains present and appropriate transcriptional elements drive GFP expression. Thus GFP is not subject to decreased fluorescence as are chemical dyes due to internalization, cell division, or cell growth. As a protein of 238 amino acid residues, GFP also has the advantage of not being transferred fortuitously from cell to cell, a property critical for the unequivocal tracing of cell lineages. Finally, GFP appears to be less phototoxic than fluorescent vital dyes, possibly because the configuration of the GFP molecule results in the generation of fewer free radical molecules upon photoexcitation (48).

For the purpose of imaging developing cells in intact tissues or cell-dense culture conditions, it would be ideal to express GFP in a large subset of cells and not in every cell. Many viral vectors based on herpes-, adeno-, and retrovirus backbones have been used to introduce reporter genes into cells in intact animals or cultured cells. However, unlike other viral systems that preferentially infect quiescent cells (40), the Moloney murine leukemia virus (MoMuLV)-based retroviral vectors selectively infect and permanently integrate into the genome of dividing cells, making possible the visualization of neuronal development from early progenitor cell stages (6, 7, 31, 40). Stable integration of the retrovirus vector into the host DNA results in the expression of reporter genes in the infected cell and all of its progeny, so long as the transcriptional elements driving expression remain active.

Retroviral vectors derived from MoMuLV and Rous sarcoma virus that encode traceable reporter genes such as β-galactosidase and human alkaline phosphatase have been used extensively to examine lineage relationships or the effects of exogenous gene expres-

[1] To whom correspondence should be addressed. Fax: (650) 725-8777. E-mail: amio@leland.stanford.edu.

0014-4886/99 $30.00

sion in mammalian and avian cells (6, 7, 22, 45, 46). Unlike the detection of catalyzed product with enzymatic reporter genes such as alkaline phosphatase or detection of protein using antibodies, the signal from each GFP molecule is not amplified. In addition, because retroviral vectors integrate only as single copies into the host genome, construction of an effective GFP retrovirus requires an enhancement in the level of expression of GFP, an enhanced ability to detect GFP fluorescence, or both. Although previous investigators have demonstrated that the expression of high levels of GFP in neurons can enable both the detection of these cells and a description of their morphological properties in tissue slices (30), these methods introduced multiple copies of the reporter GFP transgene.

Here we describe the assembly of a GFP-encoding replication-incompetent retrovirus that efficiently infects and expresses persistently in a wide range of cell types. We use this virus to infect progenitor cells of the developing rat cerebral cortex and avian embryos, to test whether the GFP can be used to image the development of cells in these disparate systems. The GFP marker expresses well in many different cell types in both species and continues to be expressed in mature neurons and glia in adult animals. In addition to employing *cis*-acting elements that should increase the transcription level of the GFP reporter, mutated or modified GFPs with improved fluorescence or altered cellular localization were developed to increase the sensitivity of detection and more effectively observe the fine cellular structures.

To overcome the problems of low viral titers, retroviral vectors were assembled and "pseudotyped" with the G envelope protein of vesicular stomatitis virus (VSV-G). Pseudotyping alters the host range of a virus by exchanging the surface antigens among both DNA and RNA viruses (49). The resulting VSV-G-pseudotyped retroviruses possess a broad host range and can be concentrated 1000-fold with minimal loss of biological activity (5, 11). We have investigated the ability of these viruses to introduce the GFP reporter vectors into a large population of cells in the developing cortex or chick neural crest and demonstrate the possibility of real-time imaging of retrovirally infected cells. The general utility of this approach is evidenced by the development of GFP-encoding retrovirus vectors designed for gene therapy (e.g., 13, 42).

MATERIALS AND METHODS

Generation of Mutated EGFP

EGFP (Clontech Laboratories, Palo Alto, CA) with S147P (mut1EGFP) or V163A and S175G (mut4EGFP) mutations were generated by oligonucleotide-directed PCR mutagenesis using *Pfu* DNA polymerase (Stratagene, La Jolla, CA) and pEGFP-1 (Clontech Laboratories, Palo Alto, CA) as template. To generate mut1EGFP, oligo1 and oligo3 were used as primers to synthesize the 5′ end of the mutant (5′mut1; see below for oligo nucleotide sequences), and oligo4 and oligo2 were used as primers to synthesize the 3′ end (3′mut1). The complete mut1EGFP was generated using oligo1 and oligo2 in a PCR with 5′mut1 and 3′mut1 as templates. To generate mut4EGFP, oligo1 and oligo5 were used as primers to generate the 5′ end of the mutant (5′mut4), and oligo6 and oligo2 were used as primers to generate the 3′ end (3′mut4). The complete mut4EGFP was generated using oligo1 and oligo4 in a PCR with 5′mut4 and 3′mut4 as templates.

PCR-generated mut1EGFP and mut4EGFP were digested with *Bam*HI and *Not*I and ligated into compatible sites in pBluescript II SK(+) (Stratagene) to generate pBSmut1EGFP and pBSmut4EGFP, which were sequenced to confirm incorporation of the mutations. All PCRs were performed for 10 cycles. Primers were oligo1, 5′-ccgggatccaccggtcgc-3′; oligo2, 5′-gatctagagtcgcggccgc-3′; oligo3, 5′-gttgtgggggttgtagttgtactc-3′; oligo4, 5′-caacccccacaacgtctatatc-3′; oligo5, 5′-gttgtggcggatcttgaagttcgccttgatg-3′; and oligo6, 5′-atccgccacaacatcgaggaccggcggcgtg-3′.

Generation of Membrane-Targeted EGFP

Oligonucleotide primers (oligo7 and oligo8; see below for sequences) homologous to the amino-terminus palmitoylation site of GAP-43 (neuromodulin) were used to generate the "gap-tag" with a PCR amplification using *Vent* DNA polymerase (New England Biolabs, Beverly, MA). The amplified gap-tag product was digested with *Bam*HI and *Eco*RV, ligated into compatible sites of pBluescript II SK(+) to generate pBS-GAP, and sequenced. To generate gapEGFP, pEGFP-1 was digested with *Nco*I, the end nucleotides were filled in using the large fragment of DNA polymerase I, and the plasmid was digested again with *Not*I to generate a 724-bp *Nco*I–*Not*I fragment encoding EGFP. This *Nco*I–*Not*I fragment was ligated together with the 75-bp *Bam*HI–*Eco*RV fragment from pBS-GAP into the *Bam*HI–*Not*I site of the 5.1-kb pCA-EGFP backbone (see below) to generate pCA-gapEGFP. The junction of the gap-tag with EGFP was sequenced to confirm the in-frame fusion of the gap-tag to EGFP. The synthesis of intact protein was also confirmed by transient transfection into NIH 3T3 cells using standard calcium phosphate transfection methods (3). Primers were oligo7, 5′-accggatccaccggtcgccaccatgctgtgctgtatgagaagaaccaaacaggttgaaaag-3′, and oligo8, 5′-caatgatatcttttggtcctcatcattcttttcaacctgtttggttct-3′.

Generation of LZRS-CA-EGFP Constructs

The cytomegalovirus enhancer and β-actin promoter (CA) were isolated from pCA-G-GFP (gift from Dr. J.

Mizuuchi, Osaka University, Japan (33)) as a 1.7-kb *Pst*I–*Sna*BI fragment and ligated into the *Pst*I–*Kpn*I site of pEGFP-1 to generate pCA-EGFP. The 740-bp *Bam*HI–*Not*I GFP-encoding fragments from pBSmut1EGFP and pBSmut4EGFP were ligated into the *Bam*HI–*Not*I site of pCA-EGFP to replace EGFP, generating pCA-mut1EGFP and pCA-mut4EGFP. To generate retroviral constructs with both the retroviral and the CA promoter elements, the approximately 2.7-kb *Eco*RI–*Not*I fragments from pCA-EGFP, pCA-gapEGFP, pCA-mut1EGFP, and pCA-mut4EGFP containing the CA transcriptional elements and GFP were ligated using *Eco*RI linkers into the *Eco*RI site of the 11.2-kb LZRS retroviral vector backbone (gift from Dr. G. Nolan, Stanford University (20)) to generate LZRS-CA-EGFP, LZRS-CA-gapEGFP, LZRS-CA-mut1EGFP, and LZRS-CA-mut4EGFP.

Generation of Retroviral Particles

Amphotropic, replication-incompetent retrovirus particles of LZRS-CA-based viruses were generated using the Phoenix helper cell line derived from a 293T human embryonic kidney transformed cell line (gift from Dr. G. Nolan, Stanford University). Briefly, retroviral constructs were introduced into Phoenix cells using standard calcium phosphate transfection protocols (3). Cells were selected for puromycin resistance. After 1 week in culture, cells were placed at 32°C, and conditioned medium was collected after 12 h and used directly to infect cells.

VSV-G-pseudotyped replication-incompetent retroviral particles were generated using the 293T-based helper cell line 293GPG (gift from Dr. R. Mulligan, Harvard University (36)). LZRS retroviral vectors were transfected into the 293GPG packaging cell line, and the pseudotyped retroviruses were collected and concentrated according to published protocols (5). Viral titers greater than 1×10^9 infectious virions/ml were obtained consistently.

Infection and Analysis of Cultured Cells

The dorsal cerebral cortex was dissected from E14 rat embryos (E0 = plug date). Cells were dissociated by trituration and plated at a density of 5×10^5 to 3×10^6 cells per milliliter onto polylysine-coated eight-chamber microscope slides (Nunc, Inc., Naperville, IL) in serum-free Neurobasal medium (Gibco BRL, Grand Island, NY). After 24 h in culture at 37°C and 5% CO_2, cells were exposed to approximately 1×10^4 infectious particles of virus and cultured for an additional 48 h. Cells were then fixed in 2% paraformaldehyde and visualized using an epifluorescence microscope (Nikon Optiphot, Japan) with a cooled CCD camera (Princeton Instruments, Trenton, NJ). To compare the levels of fluorescent signal between different cells, images were acquired using identical settings and analyzed using the OpenLab Measurement program (Improvision, UK).

Further quantitation was obtained using Abelson murine leukemia virus (AMuLV)-transformed lymphocytes (300-18 (1)) which were cultured at 37°C in 5% CO_2 in DMEM, 10% FCS (Gibco BRL). Cells (1×10^6) were infected with 5×10^4 infectious particles of amphotropic LZRS-CA-mut4EGFP. Cells expressing GFP were enriched manually 3 days after infection, and the pool of infected cells was analyzed by flow cytometry (Coulter EPICS753; Beckman Coulter, Fullerton, CA) after 1 week. Cells were excited at 488 nm, fluorescence emission was measured at 525 nm, and data analysis was performed using Elite software (Beckman Coulter).

Infection and Analysis of Developing Brain Cells

Pregnant Long–Evans rats (Simonsen, Gilroy, CA) were anesthetized with 60 mg/kg ketamine and 12 mg/kg xylazine, and intrauterine injections of the virus were performed under sterile conditions according to published protocols (7). Concentrated VSV-G pseudotyped retroviruses with a titer of approximately 1×10^8 infectious particles per milliliter were diluted approximately 1:3 into PBS containing 0.01% trypan blue and injected into the lateral ventricles of E16 embryos *in utero* using a Hamilton syringe. Animals were sacrificed at either E17 or P6 to P32. Images of layers 2/3 and 5 (Figs. 5B and 5C) were acquired at P7, because the abundance of fluorescent processes makes it difficult to identify individual axonal branches from each cell in the adult animal. Embryonic brains were fixed in 2% paraformaldehyde/0.1 M phosphate buffer and labeled cells were imaged in 50-μm sections. Postnatal embryos were analyzed either immediately after sectioning as living, 200-μm cortical slices or after fixation and subsequent sectioning of the brain into 50-μm slices. Cells were visualized using an epifluorescence microscope (Nikon Optiphot) equipped with a cooled CCD camera (Princeton Instruments) or laser confocal microscopy (Bio-Rad MRC600; Hercules, CA).

Retrograde Labeling of Brain Cells

Using a stereotaxic device, 0.1 μl of 2% Fast blue (Sigma, St. Louis, MO) was injected 0.6 mm from the pial surface into the superficial layers of P28 rat cerebral cortex previously infected with gapEGFP-expressing retrovirus. The rat was sacrificed after 4 days and the brain was fixed with 2% paraformaldehyde, sectioned into 50-μm slices, and visualized with a Nikon epifluorescence microscope. Data acquisition and analysis were performed using a cooled CCD camera (Princeton Instruments) and OpenLab image processing program (Improvision).

Infection and Analysis of Avian Embryos

Retrovirus was injected into the developing hindbrain region of chick embryos (White Leghorn; AA Laboratories, Westminster, CA) at the eight-somite stage *in ovo* under a dissecting microscope by pressure injection (Picospritzer; General Valve Corp., Fairfield, NJ). The injected eggs were then sealed and placed in a rocking incubator at 37°C for a minimum of 26 h. The infected embryos were then either placed in Neurobasal medium (Gibco BRL) with B27 supplement (Gibco BRL) and 0.5 mM L-glutamine or moved *in ovo* to an incubation chamber fitted on the microscope stage (Zeiss Axiovert10, Germany). Images of live embryos were acquired by time-lapse videomicroscopy (Bio-Rad MRC600).

Ballistic Introduction of GFP into Ferret Brain Slices

Ferret brains were removed at P14 (at stages of development equivalent to P3 in rat), sectioned into 300-μm sections, and cultured in a modified serum-free Neurobasal medium (Gibco BRL) and B27 supplement (Gibco BRL) at 37°C in 5% CO_2 on Transwell tissue culture inserts (Corning Costar, Cambridge, MA) for 24 h. Gold particles (0.6 μm) (Bio-Rad) were coated with pCA-gapEGFP and subsequently introduced into the slices using an air-pressure gun following published protocols (2, 27). Slices were incubated for an additional 24 h and then fixed in 2% paraformaldehyde.

RESULTS

Construction of the Retrovirus Backbone

The MoMuLV-based retroviral vector LZRS was used as the backbone from which to construct the vectors described here (20). We introduced additional transcriptional elements into the LZRS vector to augment the level of reporter gene expression, as the retrovirus long-terminal repeat (LTR) transcriptional element appeared to be less effective in some cells (e.g., pyramidal neurons) than in others (e.g., glia) (Weimann and McConnell, unpublished observations). This is consistent with observations by others of the variability in virus LTR activity in different cell types (32, 44).

The promoter/enhancer combination selected for use with the LZRS vector was the human cytomegalovirus enhancer coupled to the chicken β-actin promoter, a combination that is active in a number of different cell types (29, 33). The CA enhancer/promoter elements were inserted transcriptionally downstream of the 5′ LTR transcriptional elements in the LZRS retrovirus vector to generate the virus construct LZRS-CA. Sequences encoding a form of GFP (see below) were inserted transcriptionally downstream of both the MoMuLV and the CA transcriptional elements in the 5′ to 3′ orientation (Fig. 1). While we were initially concerned about the potential negative effects of an additional element on transcription from the retroviral LTR (which would affect the viral titer), titers obtained using LZRS-CA-GFP constructs harboring both the viral LTR and the CA transcriptional elements in ecotropic and amphotropic producer cell lines did not differ significantly from titers of the LZRS-GFP vectors containing only the LTR. We consistently obtained titers of approximately 10^5 to 10^6 infectious particles per milliliter of supernatant from helper cell lines transiently transfected with each of the LZRS-based vectors.

Construction of Altered GFPs

Using GFP-encoding viral vectors available at the time we initiated these studies, it was difficult to see the GFP-expressing cells using standard epifluorescence or confocal microscopy (data not shown). We therefore attempted to optimize GFP fluorescence at the protein level, not only to facilitate visualization of infected cells, but also to minimize exposure of live cells to toxic ultraviolet or laser light sources and reduce photobleaching of samples. To improve the level of obtainable fluorescence from each GFP molecule, we incorporated codon changes reported to result in enhanced stability and brightness at 37°C (S147P or V163A/S175G (19, 41)) into GFP. We worked with a version of GFP (EGFP; Clontech Laboratories (10)) in which codon usage has been optimized for expression in mammalian cells. In addition, EGFP incorporates mutations resulting in its redshifting, making it more suitable for visualization using confocal microscopy or epifluorescence using standard fluorescein isothiocyanate filters (FITC) (10).

Codon changes were introduced into EGFP by oligonucleotide-primed mutagenesis (3), and the resultant constructs were called mut1EGFP (S147P) or mut4EGFP (V163A/S175G) (Fig. 1). To generate the S147P mutation, nucleotides "agc" encoding serine at residue 147 were changed to "ccc"; to generate the V163A/175G mutations, nucleotides "gtg" encoding valine at residue 163 were changed to "gcg" and nucleotides "agc" encoding serine at residue 175 were changed to "ggc." As discussed below, the introduction of codon changes S147P or V163A/S175G further enhance the brightness of EGFP.

LZRS-CA-mutEGFP Are Brighter than LZRS-CA-EGFP

Previous studies showed that the S147P and V163A/S175G mutations confer increased fluorescence of wild-type GFP (wt GFP) in *Escherichia coli* bacteria grown at 37°C, presumably due to an enhancement of protein folding at this higher temperature relative to wt GFP (19, 41). To assess the relative fluorescence of the

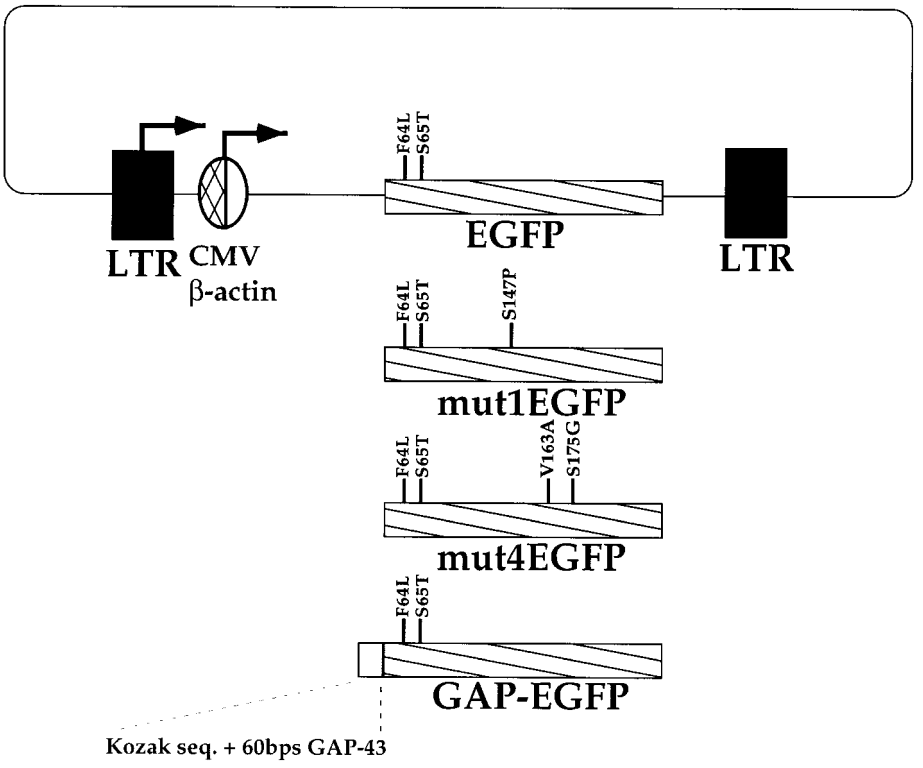

FIG. 1. Schematic of retroviral constructs. The LZRS-CA-EGFP, LZRS-CA-mut1EGFP, LZRS-CA-mut4EGFP, and LZRS-CA-gapEGFP plasmids are schematized here. The mutations noted are with respect to wt GFP amino acid sequences. The backbone of the LZRS vector is represented as a straight line; the LTR transcriptional elements are depicted as black rectangles; the CMV/β-actin enhancer/promoter is depicted as a half-hatched oval; the GFP inserts are shown as striped rectangles. The putative origins of transcription from the two promoter elements are denoted with arrows.

mutEGFPs compared with EGFP, each of the mutEGFPs was inserted in a LZRS-CA vector to generate LZRS-CA-mut1EGFP and LZRS-CA-mut4EGFP (Fig. 1), which were compared to a control vector, LZRS-CA-EGFP. The plasmid constructs were transfected into amphotropic packaging cell lines and the supernatant was applied to freshly isolated rat cortex progenitor cells from E14, which consist primarily of dividing cells.

E14 cortical progenitors were infected with retrovirus expressing EGFP or mutEGFPs 12 h after plating at an initial density of 5×10^5 cells/ml, with a low (approximately 5×10^4 infectious particles) titer of the harvested virus to ensure that cells would not fortuitously become superinfected. Cells were imaged using a cooled CCD camera 48 h postinfection (Figs. 2A–2C). The fluorescence of cells infected with each LZRS-CA-mutEGFP was measured digitally and compared to that of LZRS-CA-EGFP (Table 1). Cells infected with mut4EGFP (V163A/S175G) were approximately fourfold brighter than cells infected with LZRS-CA-EGFP, while cells infected with mut1EGFP (a and b; S147P) were approximately threefold brighter than EGFP (Figs. 2A–2C; Table 1).

LZRS-CA-mut4EGFP was also introduced by a low-titer infection into an immortalized pre-B lymphocyte cell line, 300-18 (1). Fluorescent cells were manually enriched, and the pooled population of GFP-expressing cells (as well as uninfected cells) was analyzed by fluorescent activated cell sorting (FACS). Cells infected with LZRS-CA-mut4EGFP virus (V163A/S175G) were roughly threefold brighter than cells expressing EGFP (Fig. 3).

Membrane-Targeted EGFP (gapEGFP)

To direct the transport of EGFP into the dendrites and axons of developing neurons, EGFP was tagged with 75 bp encoding the Kozak consensus sequence and the first 20 amino acids that are shared by the GAP-43 gene, including the palmitoylation sequences, to generate gapEGFP (Fig. 1) (23, 30). While the complete GAP-43 protein is localized specifically to axonal membranes, the N-terminus amino acid sequences function only to target the protein to the cell membrane; other sequences in GAP-43 are probably required to restrict the protein specifically to axons (23, 24). The N-terminus 20 amino acid sequence from GAP-43 has been shown previously to direct GFP to the membrane of mature neurons as well as other cell types (16, 30).

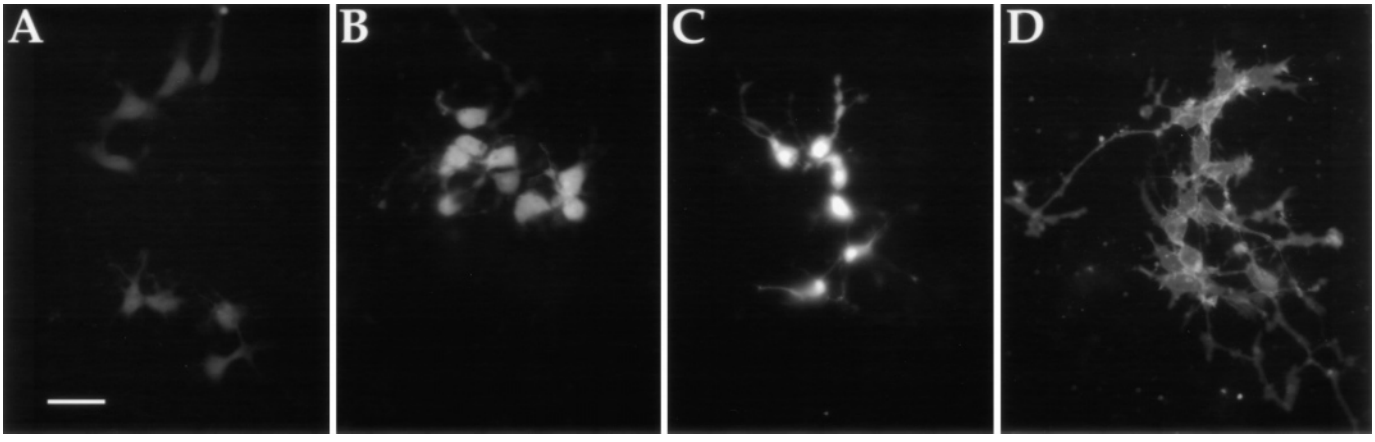

FIG. 2. Cultured cortical cells infected with GFP-encoding retrovirus. E14 rat cortical cells are shown 48 h after infection with retrovirus encoding GFP. Clones of fluorescent cells appear white among a confluent population of unlabeled cells. Cells infected with (A) LZRS-CA-EGFP, (B) LZRS-CA-mut1EGFP, (C) LZRS-CA-mut4EGFP, and (D) LZRS-CA-gapEGFP. All images were acquired and analyzed under identical conditions using a cooled-CCD camera. Scale bar, 20 μm.

We predicted that GAP-43-tagged EGFP would result in a more complete visualization of neuronal morphology compared to unlocalized GFP. GapEGFP was cloned behind the LZRS LTR and CA transcriptional elements to generate LZRS-CA-gapEGFP, and this vector was transfected into an amphotropic virus helper cell line (Phoenix; gift from G. Nolan, Stanford University). Again, E14 rat embryonic cortical cells were plated for 12 h at an initial density of 5×10^5 cells/ml and then infected with a low titer of the harvested virus. Cells were cultured in serum-free medium at high density for 2 days. Clusters of fluorescent cells were readily visible among a confluent layer of uninfected cells. The morphology of gapEGFP-labeled cells was clearly visible and included fine cellular processes (Fig. 2D), suggesting that this virus may be useful in visualizing the detailed dendritic and axonal morphologies of neuronal cells in the intact cortex. In addition these results suggest that membrane-targeted or cytoplasmic GFP may be useful for clonal analysis of cultured progenitor cells *in vitro*, including the possibility of watching clones develop over time in high-density cultures (Figs. 2A–2D).

Gross overexpression of gapEGFP can result in the accumulation of fluorescent protein within the cell: NIH 3T3 cells transfected with large copy numbers of this construct and neurons in ferret cortical slices transfected with high copy number of plasmid via particle-mediated gene transfer both amass large quantities of GFP protein in large membrane structures within the cell without showing increased levels of the fluorescent protein on the membrane (Fig. 4). GAP-43 is normally processed through the Golgi apparatus (24), and the presence of a large amount of GFP tagged with the palmitoylation signal of GAP-43 may overwhelm the sorting mechanisms within of the Golgi, resulting in protein accumulation within this organelle. Similar observations have been made in other systems in which GAP-43 or proteins containing the N-terminal sequence from GAP-43 have been overexpressed (23, 24). The levels of GFP expressed from a single copy of retrovirus (Figs. 3D and 5A–5E) are sufficient to visualize cells but do not result in the accumulation of excess GFP within the cell body.

TABLE 1

Fluorescence Signal Intensity of Cells Infected with GFP-Encoding Retrovirus

Construct	Mutation[a]	No. of cells	Fluorescence signal[b]	Relative signal[c]
LZRS-CA-EGFP	None	12	578 ± 277	1
LZRS-CA-mut1EGFP	S147P	18	1877 ± 644	3.2
LZRS-CA-mut4EGFP	V163A/S175G	10	2302 ± 981	3.9

[a] Mutations are noted with respect to EGFP.
[b] Fluorescence is measured in pixels.
[c] Relative fluorescence is calculated with respect to average signal of cells infected with LZRS-CA-EGFP.

Use of VSV-Pseudotyped LZRS CA mut4EGFP and LZRS CA gapEGFP to Introduce GFP into the Embryonic Cortex

Time-lapse videomicroscopy of fluorescently labeled cortical cells has revealed complex migration patterns of developing neurons (34, 35) and suggested that daughter cells arising from mitoses involving different cleavage planes adopt distinctive fates after cell division (8). For efficient imaging of the dynamic behavior of GFP-labeled cells developing in explant or slice preparations, many labeled cells should be visible within the microscope's field of view at 20× to 40×

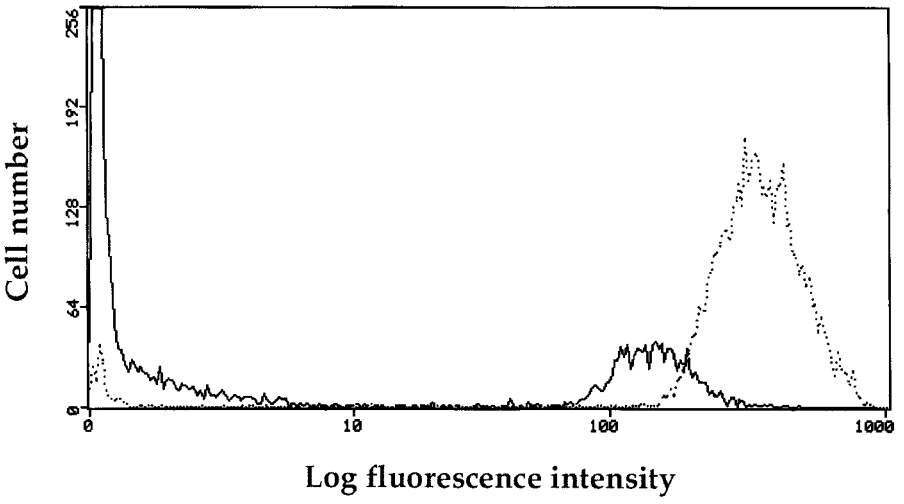

FIG. 3. FACS analysis of AMuLV cells infected with LZRS-CA-EGFP and LZRS-CA-mut4EGFP. AMuLV-transformed lymphocyte cell line 300-18 was infected with LZRS-CA-EGFP (solid line) and LZRS-CA-mut4EGFP (dashed line) and the fluorescence of the cells was plotted on a linear scale of cell number (*y* axis) to logarithmic scale of fluorescence intensity (*x* axis). 10,000 cells were acquired for both samples; the two populations contain different proportions of infected and uninfected cells.

magnification so that well-labeled cells that are active at the time of the experiment can be found in the visual field. Infection of embryonic rat brain with conventional amphotropic or ecotropic replication-incompetent retrovirus results in the labeling of up to 100 cells in each brain (J. Weimann and S. McConnell, unpublished; 39, 45, 46), numbers that are insufficient for imaging experiments. To overcome the problem of low viral titers, recombinant GFP-encoding retroviruses pseudotyped with the VSV-G protein were generated and used to infect the developing cortex.

The vesicular stomatitis virus glycoprotein recognizes membrane lipid components as receptors that mediate entry into host cells. VSV-G expressed in retrovirus helper cell lines can be used to package MoMuLV-based retrovirus to generate a polytropic, VSV-pseudotyped virus (36). These viral particles can be concentrated by centrifugation to a titer of up to 10^9 infectious particles per milliliter, a 1000-fold increase over conventional amphotropic and ecotropic retroviruses (5). Concentrated VSV-G-pseudotyped LZRS-CA-mut4EGFP or -gapEGFP retrovirus particles were thus generated and injected into the lateral ventricles of rat embryos *in utero* on E16 using modifications of published procedures (7).

Rats infected with VSV-G-pseudotyped retrovirus were sacrificed at various times between E17 and postnatal day 26. Embryonic brains were fixed in 2% paraformaldehyde and labeled cells were imaged in 50-μm sections, while postnatal embryos were analyzed either immediately after sectioning as living, 200-μm cortical slices or after fixation and subsequent sectioning of the brain into 50-μm slices. Similar numbers of cells were visible within the animals injected with the high-titer virus in each experiment. The increased viral titer, possibly in combination with the receptor target of VSV-G (see Discussion), resulted in expression of GFP in approximately 20 cells in each field of view using a 20× objective to visualize a 200-μm section of the cortex.

Cells expressing either mut4EGFP or gapEGFP were present throughout development into adulthood. At all stages of development, many different types of cells expressed the GFP reporter genes (Figs. 5A–5E). The infected cells exhibited morphologies typical of cells labeled in previous studies with a number of stains or intracellular markers (17, 18, 21, 38 and see below). In embryonic cortex, progenitor cells in the ventricular zone exhibited GFP 24 h postinfection (Fig. 5A). In more mature animals, various cell types such as pyramidal cells (in layers 2/3 and 5; Figs. 5B and 5C) and interneurons (e.g., chandelier cells; Fig. 5D) are readily distinguishable by their morphologies using the membrane-targeted GFP. The single copy of LZRS-CA-gapEGFP generated levels of fluorescence sufficient to visualize the detailed morphology of growth cones of developing neurons (Fig. 5E).

gapEGFP-Labeled Cells Appear to Make Normal Local and Long-Distance Connections

The morphologies of cells expressing gapEGFP were analyzed at various stages of development after infection into E16 rat embryos, to ascertain whether the membrane-tagging sequences or the palmitoylation of EGFP may somehow disrupt the normal development of dendrites or axons. GapEGFP-expressing cells persist through development into adulthood, and the cells

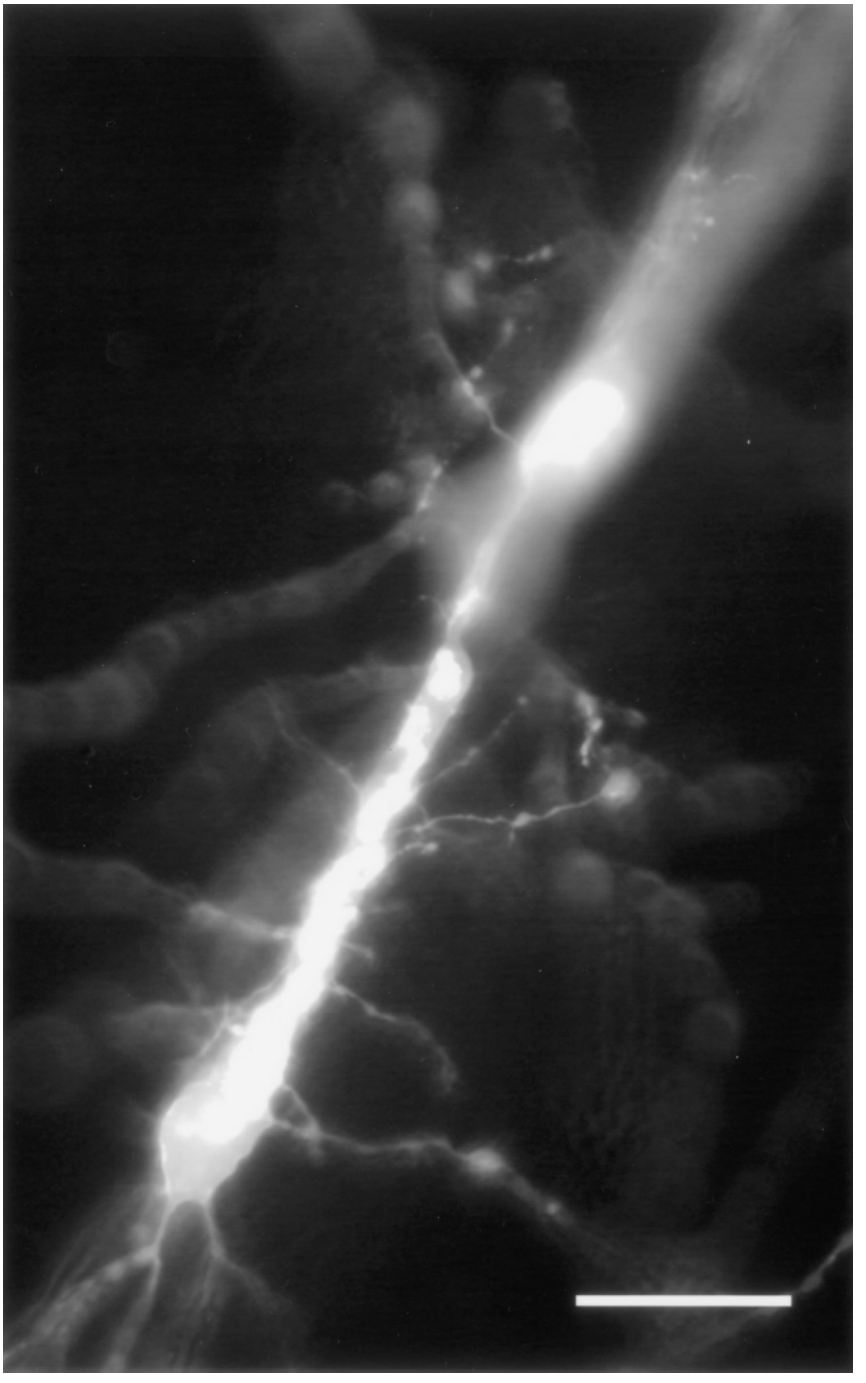

FIG. 4. CA-gapEGFP introduced into cortical slices by ballistic methods. A layer 5 pyramidal neuron transfected with pCA-gapEGFP is shown. High copy numbers of the plasmid vector encoding GFP were introduced into P14 ferret brain slices using a particle-bombardment gene delivery system (Bio-Rad). Most of the fluorescent signal appears within the cell body and within the apical dendrite. Scale bar, 20 μm.

appeared normal in several aspects: the morphologies of infected pyramidal neurons in layers 5 or 2/3 (Figs. 5B and 5C) as well as other cell types (e.g., chandelier interneurons; Fig. 5D) were similar to those analyzed by Golgi staining or filled with intracellular tracers (17, 18, 21, 38). Furthermore, layer 5 and layer 2/3 neurons expressing gapEGFP formed local dendritic or axonal branches characteristic of their normal morphology: layer 2/3 neurons elaborated dendritic and axonal branches in layer 2/3 (Fig. 5B) (21). Layer 5 neurons extended an apical dendrite to layer 1 and formed dendritic branches in 5 (Fig. 5C) (17). While local axonal projections of layer 5 pyramidal neurons appeared normal from the analysis of many different

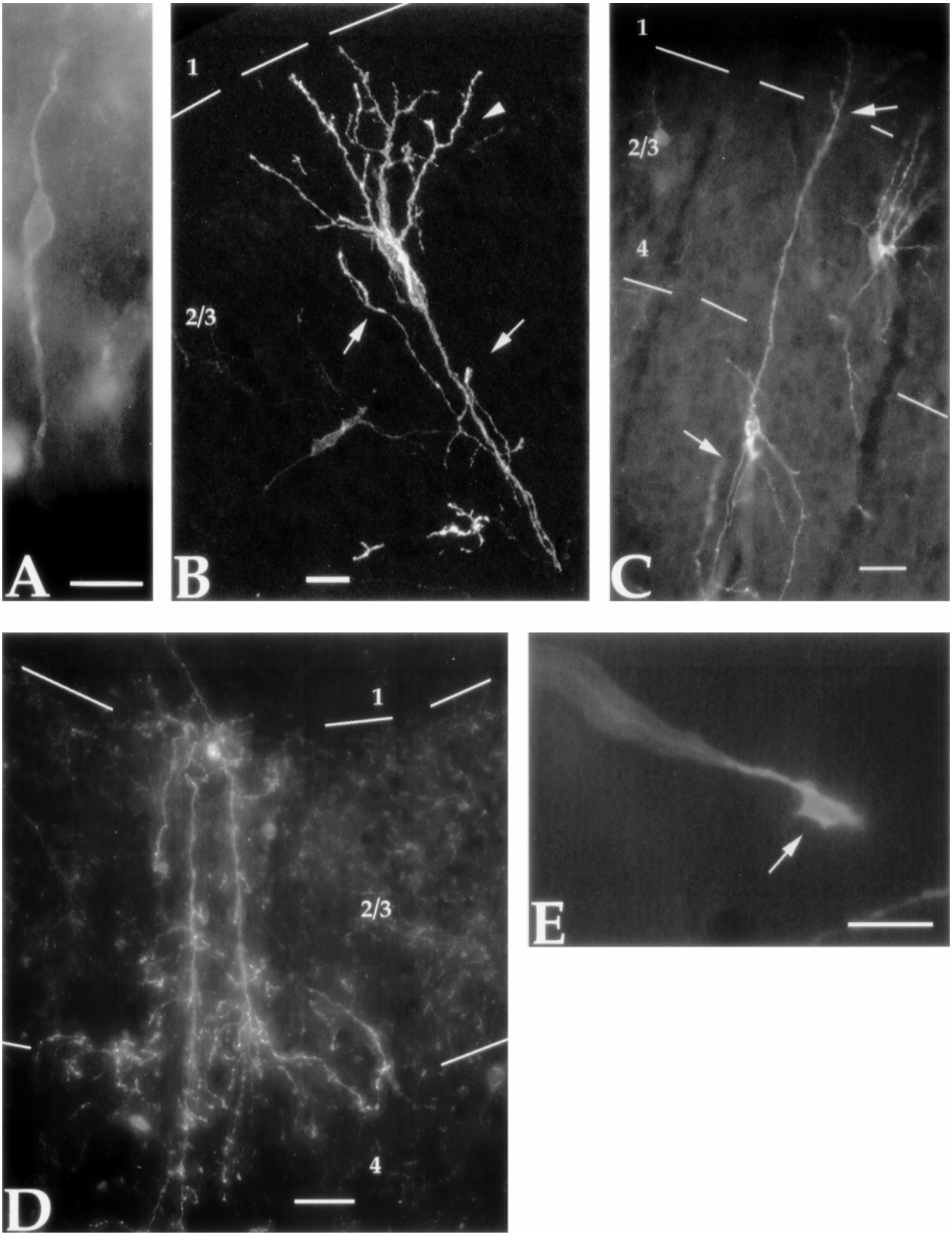

FIG. 5. Cells labeled by injection of VSV-G-pseudotyped retrovirus into embryonic cerebral cortex. E16 embryonic rat cortices were infected with LZRS-CA-gapEGFP pseudotyped retrovirus and sacrificed at various stages, and fluorescent images of gapEGFP-expressing cells were acquired. (A) Cortical progenitor cell in the ventricular zone at E17. (B) Two pyramidal cells in layer 2/3 at P7. Local axonal branches are marked by arrows. Dendritic branches in layer 2/3 are marked by arrowhead. (C) Layer 5 pyramidal neuron at P7. Dendritic branches in layers 1 and 5 are marked by arrows. (D) Chandelier neuron in layer 2/3 at P26. (E) Growth cone (arrow) in the white matter at P15. Images of live (E) or paraformaldehyde-fixed (A, B, C, D) cells were acquired using epifluorescence (A, C, D, E) or laser-confocal microscopy (B). Laminar boundaries are marked by white lines. Scale bars: (A, B) 20 μm, (C) 40 μm, (D) 50 μm, (E) 10 μm.

cells, further detailed analysis and reconstruction need to be performed to ascertain definitively whether their local projections are normal.

To investigate whether labeled neurons make long-distance axonal connections with appropriate axonal targets, we injected Fast blue (Sigma) into the left hemisphere of P28 rats that were injected previously with LZRS-CA-gapEGFP on E16. Sections from the right hemisphere were then examined 5 days after injection of the dye to see whether GFP-labeled layer 2/3 pyramidal neurons (many of which normally make connections to the contralateral cortex in rat (47)) were retrogradely labeled with the fluorescent tracer injected into the opposite hemisphere (Fig. 6). Several GFP-labeled neurons in layer 2/3 showing morphologies of pyramidal neurons were labeled with Fast blue, indicating that the cells have formed long-distance axonal connections with the contralateral cortex.

Use of VSV-Pseudotyped LZRS-CA-mut4EGFP and LZRS-CA-gapEGFP to Introduce GFP into Chick Embryos

Hindbrain rhombomeres produce neural crest cells which emigrate from the neural tube in a segmental manner (25). The vital dye DiI has been used to label and track migrating neural crest cells and show that they follow specific routes from rhombomeres 2, 4, and 6 and to a lesser extent from rhombomeres 3 and 5. To determine if the VSV-G-pseudotyped retroviruses could be used to infect and image developing avian embryos, we introduced LZRS-CA-EGFP or LZRS-CA-gapEGFP retrovirus into the hindbrain of stage 9 chick embryos *in ovo* (14). The infected embryos were then incubated on a rocking platform at 37°C.

The infected cells were imaged successfully *in vivo* using time-lapse videomicroscopy, and images from a static time point approximately 26 h after infection are presented in Figs. 7A and 7B. The infected cells appear to follow appropriate migratory routes (Fig. 7A) and undergo normal differentiation. Depending on the age of the embryo and amount of virus injected, we are able to infect from just a few cells to virtually all of the embryonic cells. These findings indicate that neither retroviral infection nor GFP has deleterious effects on the normal migration and differentiation of embryonic neural crest cells.

DISCUSSION

We have demonstrated that VSV-G-pseudotyped retrovirus vectors expressing various forms of GFP can be used to efficiently, rapidly, and permanently label developing cells in the rodent cerebral cortex and in whole avian embryos. Furthermore, by working with GFPs with mutations that favor proper folding at 37°C or by targeting the EGFP to the membrane, we have obtained sufficient signal from a single integrated copy of reporter virus to visualize fine structures in developing and mature cells using standard epifluorescence microscopy. Although we have not unequivocally determined that every GFP-labeled cell contained a single copy of the GFP reporter, a relatively small fraction of cells ($<1/100$) was infected in each experiment and the level of GFP fluorescence was similar among cells visibly

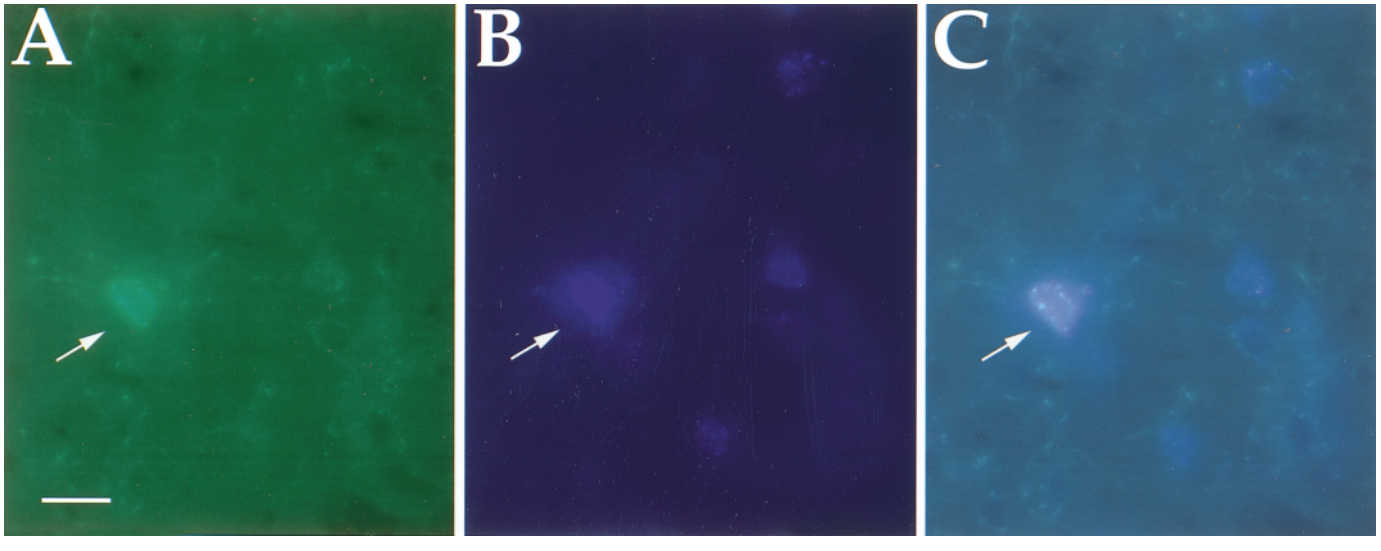

FIG. 6. Retrograde labeling of layer 2/3 cells infected with LZRS-CA-gapEGFP. Rat embryos injected with LZRS-CA-gapEGFP at E16 were injected with Fast blue (Sigma) in the right hemisphere at P28. GapEGFP-expressing layer 2/3 neurons in the left hemisphere were analyzed for cytoplasmic presence of Fast blue. (A) GFP-labeled neurons visualized with an FITC filter (480 nM). (B) Cells labeled with Fast blue visualized using an ultraviolet filter (400 nM). (C) Overlay of (A) and (B). Double-labeled cell is marked with arrowhead. Scale bar, 20 μm.

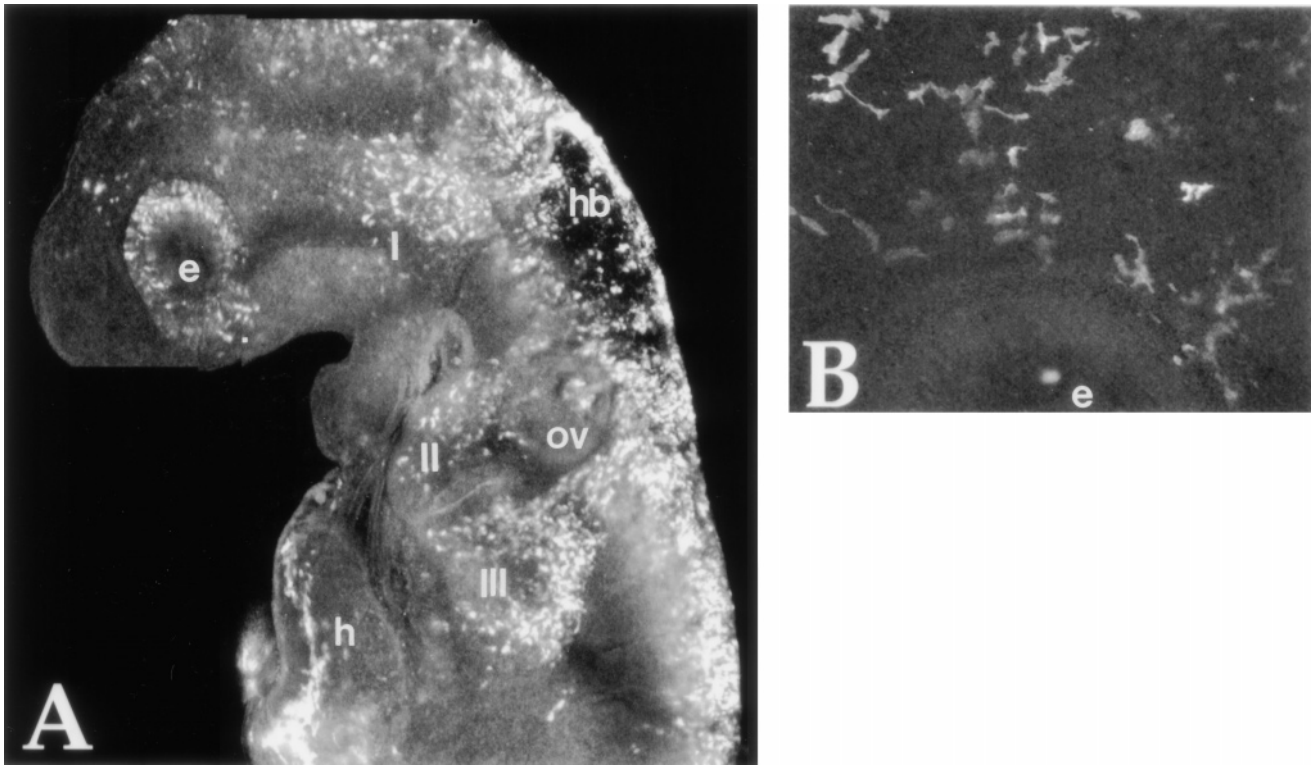

FIG. 7. Neural crest cells labeled by injection of VSV-G-pseudotyped retrovirus into hindbrain of embryonic chicks. Chick embryos received injections of GFP-expressing retrovirus into the hindbrain at the eight-somite stage. Embryos were then allowed to mature for 26 h. Cells expressing GFP appear white and are seen to have emigrated from the hindbrain along appropriate migratory routes. (A) Whole chick embryo infected with LZRS-CA-EGFP. Abbreviations: e, eye; h, heart; hb, hindbrain; ov, otic vescicle; I, II, and III, pharyngeal arches. (B) High magnification of head mesenchyme of chick embryo infected with LZRS-CA-gapEGFP. Abbreviations: e, eye.

expressing the protein, leading us to conclude that superinfection of virus did not occur.

VSV-pseudotyped retrovirus particles can be concentrated up to 1000-fold by centrifugation, enabling the introduction of GFP reporters into large numbers of cells in intact animals. These advances are critical for the use of GFP for live imaging in cortical explants or slices and in whole avian embryos, as well as in various other tissues and organisms. VSV-G-pseudotyped retroviruses employ membrane lipids as receptors, which may contribute to their efficient incorporation into various cell types. Cortical progenitor cells form an epithelial sheet that lines the lateral ventricles of the brain (4). These cells are highly polarized in terms of protein composition at the apical versus basolateral surface (9), with only a small portion of each cell's apical membrane (1–2 μm in diameter) contacting the ventricle (9, 15), forming the "delivery surface" for viral infection. Because VSV-G-pseudotyped retroviruses use lipid components of the membrane such as phosphatidylserine as a receptor (26), it is possible that these viruses enter the polarized progenitor cells via their small apical surface more efficiently than do viruses with standard ecotropic or amphotropic envelope proteins which recognize protein components (such as basic amino acid or phosphate transporters (28)) to enter cells.

One possible consequence of the efficient entry of VSV-G-pseudotyped retrovirus into cortical progenitors is reflected in the detection of EGFP-labeled layer 5 pyramidal neurons in animals following injections at E16. Birth-dating data suggest that E16 progenitor cells produce the last layer 5 neurons of the cortex (12). The ability of virus to infect this population suggests that viral entry and integration must occur very rapidly after injection of virus into embryos. We have not observed labeled layer 5 neurons after infection of E16 cortex using retroviruses packaged with standard ecotropic or amphotropic host range envelope proteins.

Cells expressing the mutated or membrane-targeted forms of EGFP persist through development, and while we have not recorded the total numbers of infected cells in each brain, the approximate numbers of cells per brain during development appear similar between experiments, suggesting that the transcriptional elements remain active through development and that there is not a significant selection against cells expressing either mut4EGFP or gapEGFP. Neurons and glia infected with LZRS-CA-gapEGFP express sufficient GFP signal on the surface to clearly reveal the cell's

morphology. These cells do not, however, show evidence of the accumulation of unprocessed protein in the Golgi apparatus, as do cells transfected with multiple copies of gapEGFP. The continued presence of virally infected gapEGFP cells into adulthood, the apparently normal morphology of labeled cells, and the efficient targeting of EGFP to the cell membrane suggest that labeled cells can maintain normal properties following expression of gapEGFP from the retrovirus.

In summary, the EGFP retroviruses reported here provide a method with which to visualize the dynamic behaviors of developing cells *in situ*. We have generated mutations in EGFP that are severalfold brighter at 37°C than EGFP, which would facilitate imaging of cells in higher vertebrates. The transcriptional elements used to drive GFP expression in these viruses are active in cells of the cerebral cortex and neural crest shortly after infection and appear to remain active throughout the development of the organism. The activity of the transcriptional elements, in combination with the membrane targeting of GFP, permits us to visualize the complex morphology of a wide range of developing cells including the various neuronal cell types present in the cerebral cortex, as well as glia. By pseudotyping the retrovirus with the VSV-G protein, we can obtain high viral titers to infect a large population of dividing cells in the intact organism. Finally, the use of VSV-G-pseudotyped viruses broadens the range of species that can be infected by these retroviral vectors, enabling the study of developmental processes in organisms ranging from fish to birds to mammals.

As a word of caution, the broad host range of the pseudotyped virus that makes it a versatile and useful reagent also makes it potentially dangerous, since VSV-pseudotyped virus can also readily infect humans. For this reason, pseudotyped virus should not be used to express sequences known to be oncogenes. Work using the virus should be conducted in appropriate facilities and measures to contain live virus should be exercised to prevent any exposure while handling and disposing of the virus.

ACKNOWLEDGMENTS

We thank Chris Kaznowski for technical assistance, Allison Hall for preparation of ferret brain slices, and Catherine Carswell Crumpton for performing the FACS analysis. This work was supported by ACS PF4263 to A.O., NIH EY08411 and NS12151 to S.K.M., NIH MH49176 to S.E.F., and a Caltech Biology Fellowship to R.D.L.

REFERENCES

1. Alt, F. W., N. Rosenberg, S. Lewis, E. Thomas, and D. Baltimore. 1981. Organization and reorganization of immunoglobulin genes in A-MULV-transformed cells: Rearrangement of heavy but not light chains. *Cell* **27:** 381–390.
2. Arnold, D., L. Feng, J. Kim, and N. Heintz. 1994. A strategy for the analysis of gene expression during neuronal development. *Proc. Natl. Acad. Sci. USA* **91:** 9970–9974.
3. Ausubel, F. M., R. Brent, R. E. Kingston, D. D. Moore, J. G. Seidman, J. A. Smith, and K. Struhl, Eds. 1994. *Current Protocols in Molecular Biology*. Wiley, New York.
4. Bayer, S. A., and J. Altman. 1991. *Neocortical Development*. Raven Press, New York.
5. Burns, J. C., T. Friedmann, W. Driever, M. Burrascano, and J.-K. Yee. 1993. Vesicular stomatitis virus G glycoprotein pseudotyped retroviral vectors: Concentration to very high titer and efficient gene transfer into mammalian and nonmammalian cells. *Proc. Natl. Acad. Sci. USA* **90:** 8033–8037.
6. Cepko, C. L., S. Fields-Berry, E. Ryder, C. Austin, and J. Golden. 1998. Lineage analysis using retroviral vectors. *Curr. Top. Dev. Biol.* **36:** 51–74.
7. Cepko, C. L., E. F. Ryder, C. P. Austin, C. Walsh, and D. M. Fekete. 1993. Lineage analysis using retrovirus vectors. *Methods Enzymol.* **225:** 933–960.
8. Chenn, A., and S. K. McConnell. 1995. Cleavage orientation and the asymmetric inheritance of Notch 1 immunoreactivity in mammalian neurogenesis. *Cell* **82:** 631–641.
9. Chenn, A., Y. A. Zhang, B. T. Chang, and S. K. McConnell. 1998. Intrinsic polarity of mammalian neuroepithelial cells. *Mol. Cell. Neurosci.* **11:** 183–193.
10. Cormack, B. P., R. Valdivia, and S. Falkow. 1996. FACS-optimized mutants of the green fluorescent protein (GFP). *Gene* **173:** 33–38.
11. Emi, M., T. Friedmann, and J. Yee. 1991. Pseudotpe formation of murine leukemia virus with the G protein of vesicular stomatitis virus. *J. Virol.* **1202:** 1202–1207.
12. Frantz, G. D., A. P. Bohner, R. M. Akers, and S. K. McConnell. 1994. Regulation of the POU domain gene SCIP during cerebral cortical development. *J. Neurosci.* **14:** 472–485.
13. Grignani, F., T. Kinsella, A. Mencarelli, M. Valtieri, D. Riganelli, F. Grignani, L. Lancrancone, C. Peschle, G. P. Nolan, and P. G. Pelicci. 1998. High-efficiency gene transfer and selection of human hematopoietic progenitor cells with a hybrid EBV/retroviral vector expressing the green fluorescent protein. *Cancer Res.* **58:** 14–19.
14. Hamburger, V., and H. L. Hamilton. 1951. A series of normal stages in the development of the chick embryo. *J. Morphol.* **88:** 49–92.
15. Hinds, J. W., and T. L. Ruffett. 1971. Cell proliferation in the neural tube: An electron microscopic and Golgi analysis in the mouse cerebral vesicle. *Z. Zellforsch.* **115:** 226–264.
16. Jiang, W., and T. Hunter. 1998. Analysis of cell-cycle profiles in transfected cells using a membrane targeted GFP. *Biotechniques* **24:** 348–354.
17. Kasper, E. M., A. U. Larkman, J. Lubke, and C. Blakemore. 1994. Pyramidal neurons in layer 5 of the rat visual cortex. I. Correlation among cell morphology, intrinsic electrophysiological properties, and axon targets. *J. Comp. Neurol.* **339:** 459–474.
18. Kawaguchi, Y., and Y. Kubota. 1997. GABAergic cell types and their synaptic connections in rat frontal cortex. *Cereb. Cortex* **7:** 476–486.
19. Kimata, Y., M. Iwaki, C. R. Lim, and K. Kohno. 1997. A novel mutation which enhances the fluorescence of green fluorescent protein at high temperatures. *Biochem. Biophys. Res. Commun.* **232:** 69–73.
20. Kinsella, T. M., and G. P. Nolan. 1996. Episomal vectors rapidly and stably produce high-titer recombinant retrovirus. *Hum. Gene Ther.* **7:** 1405–1413.
21. Larkman, A. U., and A. Mason. 1990. Correlations between morphology and electrophysiology of pyramidal neurons in

slices of rat visual cortex. I. Establishment of cell classes. *J. Neurosci.* **10:** 1407–1414.

22. Lemischka, I. R. 1991. Clonal, in vivo behavior of the totipotent hematopoietic stem cell. *Semin. Immunol.* **3:** 349–355.
23. Liu, Y., D. A. Fisher, and D. R. Storm. 1993. Analysis of the palmitoylation and membrane targeting domain of neuromodulin (GAP-43) by site-specific mutagenesis. *Biochemistry* **32:** 10714–10719.
24. Liu, Y., D. A. Fisher, and D. R. Storm. 1994. Intracellular sorting of neuromodulin (GAP-43) mutants modified in the membrane targeting domain. *J. Neurosci.* **14:** 5807–5817.
25. Lumsden, A., and R. Keynes. 1989. Segmental patterns of neuronal development in the chick hindbrain. *Nature* **337:** 424–428.
26. Mastromarino, P., C. Conti, P. Goldoni, B. Hautecoeur, and N. Orsi. 1987. Characterization of membrane components of the erythrocyte involved in vesicular stomatitis virus attachment and fusion at acidic pH. *J. Gen. Virol.* **68:** 2359–2369.
27. McAllister, A. K., D. C. Lo, and L. C. Katz. 1995. Neurotrophins regulate dendritic growth in developing visual cortex. *Neuron* **15:** 791–803.
28. Miller, A. D. 1996. Cell-surface receptors for retroviruses and implications for gene transfer. *Proc. Natl. Acad. Sci. USA* **93:** 11407–11413.
29. Miyazaki, J., S. Takaki, K. Araki, F. Tashiro, A. Tominaga, K. Takatsu, and K. Yamamura. 1989. Expression vector system based on the chicken β-actin promoter directs efficient production of interleukin-5. *Gene* **79:** 269–277.
30. Moriyoshi, K., L. J. Richards, C. Akazawa, D. D. M. O'Leary, and S. Nakanishi. 1996. Labeling neuronal cells using adenoviral gene transfer of membrane-targeted GFP. *Neuron* **16:** 255–260.
31. Mulligan, R. C. 1993. The basic science of gene therapy. *Science* **260:** 926–932.
32. Naviaux, R. K., and I. M. Verma. 1992. Retroviral vectors for persistent expression *in vivo. Curr. Opin. Biotechnol.* **3:** 540–547.
33. Niwa, H., K. Yamamura, and J. Miyazaki. 1991. Efficient selection for high-expression transfectants with a novel eukaryotic vector. *Gene* **108:** 193–200.
34. O'Roarke, N. A., A. Chenn, and S. K. McConnell. 1997. Postmitotic neurons migrate tangentially in the cortical ventricular zone. *Development* **124:** 997–1005.
35. O'Roarke, N. A., D. P. Sullivan, C. E. Kaznowski, A. A. Jacobs, and S. K. McConnell. 1995. Tangential migration of neurons in the developing cortex. *Development* **121:** 265–2176.
36. Ory, D. S., B. A. Neugeboren, and R. C. Mulligan. 1996. A stable human-derived packaging cell line for production of high titer retrovirus/vesicular stomatitis virus G pseudotypes. *Proc. Natl. Acad. Sci. USA* **93:** 11400–11406.
37. Phillips, G. N. J. 1997. Structure and dynamics of green fluorescent protein. *Curr. Opin. Struct. Biol.* **7:** 821–827.
38. Ramon y Cajal, S. 1911. *Histologie du Systeme Nervex de l'Homme et des Vertebres.* Maloine, Paris.
39. Reid, C. B., I. Liang, and C. Walsh. 1995. Systematic widespread clonal organization in cerebral cortex. *Neuron* **15:** 299–310.
40. Robbins, P. D., H. Tahara, and S. C. Ghivizzani. 1998. Viral vectors for gene therapy. *Trends Biotechnol.* **16:** 35–40.
41. Siemering, K. R., R. Golbik, R. Sever, and J. Haseloff. 1996. Mutations that suppress the thermostability of green fluorescent protein. *Curr. Biol.* **6:** 1653–1663.
42. Stauber, R. H., K. Horie, P. Carney, N. I. Hudson, G. A. Tarasova, G. A. Gaitanaris, and G. N. Pavlakis. 1998. Development and applications of enhancer green fluorescent protein mutants. *Biotechniques* **24:** 462–471.
43. Tsien, R. Y. 1998. The green fluorescent protein. *Annu. Rev. Biochem.* **67:** 509–544.
44. Vernet, M., and J. Cebrian. 1996. Cis-acting elements that mediate the negative regulation of Moloney murine leukemia virus in mouse early embryos. *J. Virol.* **70:** 5630–5633.
45. Walsh, C., and C. L. Cepko. 1988. Clonally related cortical cells show several migration patterns. *Science* **241:** 1342–1345.
46. Walsh, C., and C. L. Cepko. 1992. Widespread dispersion of neuronal clones across functional regions of the cerebral cortex. *Science* **255:** 434–440.
47. Wise, S. P., and E. G. Jones. 1976. The organization and postnatal development of the commissural projection of the rat somatic sensory cortex. *J. Comp. Neurol.* **168:** 313–343.
48. Yang, F., L. G. Moss, and G. N. J. Phillips. 1996. The molecular structure of green fluorescent protein. *Nat. Biotechnol.* **14:** 1246–1251.
49. Zavada, J. 1982. The pseudotyping paradox. *J. Gen. Virol.* **63:** 15–24.